SSRG International Journal of Electrical and Electronics Engineering
ISSN: 2348-8379/ https://doi.org/10.14445/23488379/IJEEE-V12I10P112

Volume 12 Issue 10, 157-169, October 2025

Original Article

Assessing and Modelling the Impacts of Temperature, Cloud Cover and Relative Humidity on Global Solar Radiation: A Case Study in Ethiopia

Abera Jote Lidate[1*], A Venkata Ramayya[1], Getachew Biru Worku[2], and Tefera Terefe Yetayew[3]

[1]*Jimma University, Sustainable Energy Engineering, Jimma, Ethiopia.*
[2]*Jimma University, Institute of Technology, Sustainable Energy Engineering, Jimma, Ethiopia.*
[3]*ACE-ESD, College of Science and Technology, University of Rwanda, Rwanda.*
[4]*Adama Science and Technology University, School of Electrical and Computer Engineering, Adama, Ethiopia*

[*]*Corresponding Author : jotekalkidan061@gmail.com*

Received: 08 August 2025 Revised: 10 September 2025 Accepted: 10 October 2025 Published: 30 October 2025

Abstract *- Understanding the influence of climatological factors on solar energy is crucial for optimizing solar potential assessment, power generation, and load variation analysis. Despite Ethiopia's significant solar energy potential, the impacts of key climatic variables such as temperature (TΔ, Ta, Tmax), Cloud Cover (CC), and Relative Humidity (RH) fluctuations on Global Horizontal Irradiance (GHI) remain understudied, particularly in remote regions. This research bridges this gap by evaluating how these factors affect GHI distribution across Ethiopia. The study employs a multiple linear regression model, integrating seasonal climatic parameters with a Prescott sunshine-based model to predict GHI. Additionally, spatial interpolation via ArcGIS mapping analyzes the variations in cloud cover (35 sites of NASA data and nine sites from meteorological data), and relative humidity of (26 sites of meteorological data) against 73 sites' solar radiation patterns. Key uniqueness includes the integration of multi-climatic predictors on solar modeling and a spatially explicit assessment of Ethiopia's solar potential under varying weather conditions. Results reveal that monthly average solar irradiance ranges from 3.56 kWh/m²/day (July, Awasa) to 6.78 kWh/m²/day (February, Mekele). When climatic factors (Ta, RH, CC) are incorporated, predicted GHI varies between 3.81 kWh/m²/day (July, Jimma) and 6.59 kWh/m²/day (February, Bahir Dar). The model demonstrates high accuracy, with a multiple correlation coefficient of R = 0.999 Awasa. Statistical validation confirms robustness, showing minimal errors. Mean Bias Error (MBE: (-0.65 to -0.48) kWh/m²/day; Mean Absolute Percentage Error MAPE: (0.004–0.344%). Spatial analysis indicates that cloud cover and RH reduce GHI in western, southwestern, and central highlands, whereas drier northeastern/southeastern regions receive higher radiation. The discussion underscores the implications for PV system sizing, energy demand management, and equipment selection based on climate-solar relationships. In conclusion, this study provides critical insights into Ethiopia's solar energy dynamics, emphasizing the need for climate-informed solar planning. The findings support policymakers and energy developers in optimizing solar resource utilization under varying meteorological conditions.***

Keywords *- Climatological impacts, Solar radiation, Prediction, Multiple linear regressions, Spatial interpolation.*

1. Introduction

Solar energy is a clean, cost-effective, and abundant resource [1-3] that is crucial for power generation and heating/cooling applications in residential, commercial, and industrial sectors [4, 5]. However, its availability is influenced by climatic variations. Climate change is significantly altering global patterns of solar irradiance and Photovoltaic (PV) power generation, necessitating adaptive energy planning[6-9]. When solar radiation reaches a specific location on Earth, climatic variables such as cloud cover, relative humidity, aerosols, and precipitation significantly impact its intensity. This attenuation ultimately determines the magnitude of incoming solar energy and, consequently, the potential for energy generation at a given site [10]. Prior studies indicate that approximately 30% of incoming solar radiation is reflected back into space, while another 20% is absorbed by atmospheric components, including clouds, precipitation, and humidity [11]. Harnessing solar energy is a key challenge in developing countries, like Ethiopia, due to irregular weather conditions that affect solar radiation data. Additionally, the other basic challenges include the inadequacy of existing weather monitoring stations, a lack of measuring devices, and high costs associated with equipment, maintenance, and calibration [12]. In response to these challenges, researchers

have made significant efforts to develop theoretical models to estimate solar irradiance since the early 20th century, especially in the absence of reliable measuring tools under fluctuating weather conditions. These models use computational correlations between easily accessible climatic variables and solar radiation to design and simulate solar energy systems. Relative sunshine duration is broadly considered one of the best universally accepted parameters for assessing solar irradiance among various correlations. A contemporary focus lies on assessing how climate change alters solar radiation patterns [13]. The sunshine-based models [14-18], employing linear, quadratic, cubic, and exponential techniques, have been used in different countries and locations to predict solar radiation. Statistical analyses suggest that quadratic and cubic models offer the best fit for estimating the solar energy model. The sunshine-based models by Bahel and Ogelman have been suggested for predicting average daily and monthly Global Horizontal Irradiance (GHI), exceeding the Bristow-Campbell temperature model [10, 19]. Similarly, the Liu and Jordan model, which combines three climatic variables, overtakes temperature-based models based on the results of statistical tests [20-23].

The development of empirical models for solar radiation has progressed from basic sunshine-duration correlations to advanced machine learning algorithms. Techniques like Artificial Neural Networks (ANNs) and Wavelet Regression (WR), and Back Propagation Algorithms are now employed to forecast solar radiation by leveraging various climatic variables as inputs [24-26]. The other studies also specifically assess spatiotemporal climatic variations and their influences on average monthly and annual solar radiance through spatial interpolation techniques. These techniques have been used to predict various climatic variables and solar radiation, visualized through color maps and legend values across study areas. These comparisons often involve measured and predicted values using the Inverse Distance Weighting (IDW) method [27, 28]. The evaluation analysis indicates that the preference of Kriging over IDW has been made in studies on rainfall interpolation [29, 30], while the supremacy of IDW against Kriging methods in temperature interpolation and solar exploration [31, 32], with validation performed using RMSE, MAPE, and other statistical indicators.

Research has explored the correlation between climatic variables, such as temperature, aerosols, and cloud cover, along with solar radiation and Photovoltaic (PV) energy output. Studies indicate that under high-emission scenarios scenario Shared Socioeconomic Pass way (SSP585), the climatic effects of elevated temperatures reduce both solar radiation and PV energy generation compared to medium-emission scenarios like SSP245 [9]. The climatic impact, however, varies significantly by region. In China, for instance, the diverse solar irradiance landscape is projected to see a slight national increase (1.4 W m^{-2} per decade under SSP1-2.6) due to reduced aerosols, potentially boosting solar capacity in the southeast by approximately 4% [40]. Conversely, West Africa is projected to experience a substantial decline of around 12% in irradiance and PV output, particularly in the south, driven by increased cloud cover, aerosols, and rising temperatures [41]. Similarly, other regions, including India, North America, and Australia, are expected to face significant reductions (6-10%) in solar potential primarily due to increased cloud cover.

Several studies have focused on integrating temperature and relative humidity to forecast solar radiation using regression methods [9, 33]. Statistical analysis of Mean Bias Error (MBE) and Mean Percentage Error (MPE) has shown that these models provide long-term performance understandings, with negative and positive values, while the Root Mean Square Error (RMSE) provides short-term performance metrics, yielding positive values [9]. The other statistical analyses revealed that ambient temperature is more powerfully interrelated with solar PV output than relative humidity, making it a better predictor for PV system performance [33, 34]. Furthermore, during the wet season, high relative humidity correlates negatively with global solar radiation, while in the dry season, higher mean air temperatures are positively correlated with higher solar radiation. This trend was observed in the Hargreaves-Samani model in Ikeja, Lagos State, Nigeria [35]. The impact of relative humidity is more prominent in the summer than in the winter. Statistical analysis of temperature (TΔ) and Relative Humidity (RH) using linear, square, quadratic, cubic, and logarithmic regression techniques in MATLAB's curve fitting tool indicated that relative humidity has a greater influence on global solar radiation than mean air temperature, similar to findings in Chennai, India, during the month of July [1]. Another study examined the relationship between temperature and relative humidity with global solar radiation using the Detrended Cross-Correlation Coefficient (ρDCCA) and Multiple Detrended Cross-Correlation Coefficient (DMCx2) at three meteorological stations in Brazil. The Detrended cross-correlation revealed that the relative humidity and solar radiation were negatively correlated, while temperature and solar radiation were positively correlated [36].

Several studies have examined the significant impact of cloud cover and relative humidity on solar radiation, often analyzed using regression techniques. The statistical analysis typically indicates that the lowest values of MBE and MAPE are used to select appropriate models for solar energy system design in the study area [9]. Another study investigated the effects of cloud cover on sunshine, rainfall, humidity, and temperature at 13 stations in Bangladesh. The statistical analysis showed that the Random Effect Model (REM) showed that rainfall and humidity positively impacted cloud cover, while temperature and solar radiation had a negative impact, with temperature being insignificant [9]. Other studies have demonstrated that cloud cover influences both the magnitude and distribution of solar radiation, as seen in

Urumqi City, a semi-arid region in northwest China [9]. Research has also shown that Dye-Sensitized Solar Cell (DSC), Organic Solar Cell (OSC) technologies perform better than Crystalline Silicon (c-Si), Multi-Crystalline Silicon (mc-Si), and Copper Indium Gallium Selenide (CIGS), Building Integrated Photovoltaic (BIPV) technologies in terms of their efficiency and infrared solar radiation magnitude when cloud cover effect is considered [53]. These studies highlight the effects of cloud cover on solar radiation entering photovoltaic systems, particularly in building skin [41, 42, 53].

Globally, most prior studies provide greater emphasis on the impacts of climatic variables on solar irradiance and Photovoltaic (PV) energy production. In Ethiopia, the impact of climatic variability on solar radiation has not been comprehensively assessed. Existing research has primarily focused on developing and validating solar radiation estimation models using statistical methods and recent technologies for specific locations [18, 22, 25, 43-45]. The uniqueness of this research lies in its investigation of how specific climatic variables, such as cloud cover, relative humidity, and temperature, affect solar radiation patterns across both proximate and remote regions of the country. This study aims to bridge this gap by developing multiple regression models and applying spatial interpolation to quantify the influence of these parameters on global solar radiation. Assessing and modeling these impacts is a critical research area with substantial implications for renewable energy development, understanding climate change variations, and promoting sustainable development. By integrating advanced modeling techniques and a comprehensive assessment framework, this research will enable more accurate and reliable estimation of solar resources across diverse geographical and climatic zones. Using correlation analysis, statistical error testing, and spatial interpolation, the study provides a broad assessment of climatic drivers and their impact on solar irradiance, thereby addressing a critical uncertainty in the region's climate response. Ultimately, this work supports the effective harnessing of solar energy in Ethiopia.

2. Methodology and Materials

2.1. Study Area

Ethiopia is situated in East Africa between 3° and 15° N latitude and 33° and 48 ° °E longitudes. Climatological data, including average temperature, average relative humidity, mean cloud cover, sunshine hour duration, and geographical (latitude, longitude, altitude), were collected from meteorological stations across the country over a 13-year period (2010-2022). The national meteorological network comprises 735 class A and 283 class B functional stations, as indicated in Figure 1. The multiple linear regressions correlates the climatic variables versus GHI focuses on nine key meteorological stations across Ethiopia, representing major regions: the South and Southwest (Hawassa, Jimma, Nekemte), the Central Highlands (Addis Ababa, Adama), south east (Robe), and the Northern zone (Bahir Dar, Mekele) based on their climatic factor versus GHI, while, the Spatiotemporal variability of the cloud cover and relative humidity data set versus solar irradiance distributions pattern on climatic-solar ArcGIS map of Ethiopia. In this regard, 44 sites of cloud cover data, as well as 26 locations of meteorological relative humidity data, were compared with global horizontal irradiance data across 73 sites.

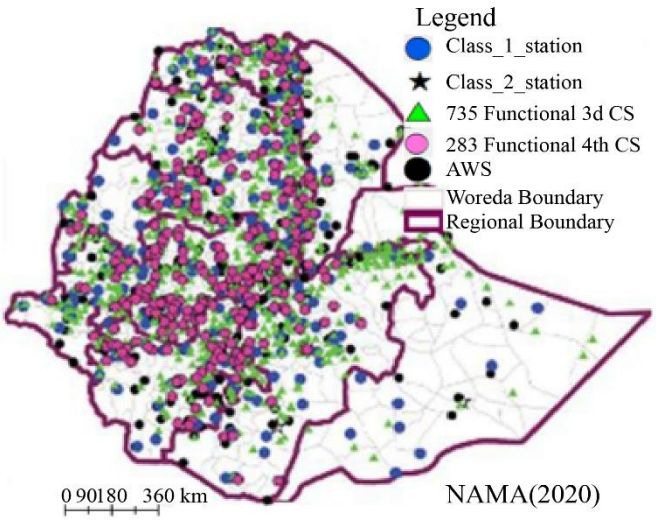

Fig. 1 Functional meteorological station [46]

2.2. Proposed Algorithm

This study involves different procedures. In 1st step, the sunshine model incorporates declination angle (δ), hour angle (ω_s), latitude (θ), extraterrestrial solar radiation (H_0), relative sunshine duration (S/S_o), and constant coefficients (a,b) to compute the solar potential at nine stations across the country. In the 2nd stage, the various combinations of average temperature (Ta), Mean Relative Humidity (RH), and average Cloud Cover (CC) of climatic variables are correlated with computed solar irradiance and its clearance index (H/H_o) to develop regression models and predict the solar potential utilizing multiple linear regression techniques, as shown in Figure 2. In 3rd stage, a statistical comparison was conducted between the computed and predicted global horizontal irradiance to assess the model's accuracy and performance using testing error metrics. In the 4th stage, the study evaluated the effect of climatic variables versus solar radiation, considering the change values between computed and predicted GHI, coefficients of developed regression equations at the 2nd step, and their error matrices at the 3rd stage. Finally, the spatial interpolation via ArcGIS climatic-solar mapping analyzes the variations of 44 cloud cover data and 26 relative humidity of meteorological data. Against 73 solar radiation data were comprehensively compared and examined to determine the climatic effects on GHI, thereby providing a geographical representation of the variability of climatic factors versus solar distribution across the country.

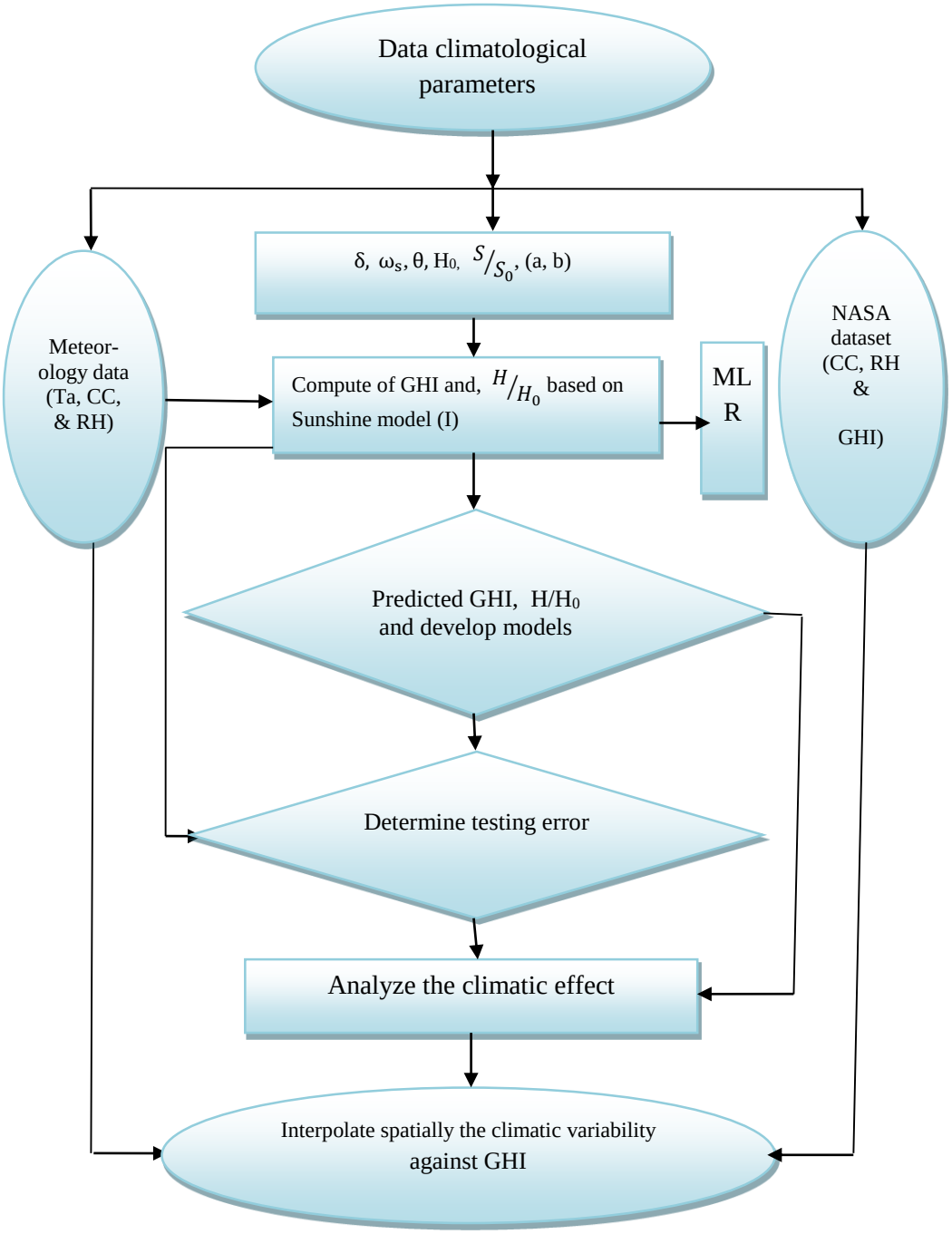

Fig. 2 Flowchart of proposed algorithm

2.2.1. Mathematical Modelling Algorithm

The Global Horizontal Irradiance was computed using sunshine duration and geographical variables based on a sunshine-based model. Multiple Linear Regressions (MLR) analysis was employed to correlate the combined effects of temperature, relative humidity, and cloud cover with the computed solar radiation and clearness index. Statistical parameters were used to validate the accuracy of the sunshine-based model. Spatial interpolation techniques were presented to correlate various climatic variables with the shine model.

Prescott Sunshine Model

The global solar irradiance is computed based on the Prescott shine model as follows: The declination angle, Equation 1 [17, 47], is

$$\delta = 23.45 \sin\left(\frac{2*\pi(203+n_d)}{365}\right) \quad (1)$$

Where (δ) declination angle (°) and n_d It is the day of the year, starting from January 1 until December 31. The hour angle is given in Equation 2 [48, 50, 51] as

$$\omega_s = cos^{-1}(-tan\,\theta\,tan\,\delta) \quad (2)$$

Extraterrestrial solar radiation (H_0) at solar constant, G_{sc}= 1367 W/m^2, latitude (θ), declination angle (δ), and hour angle (ω_s) is given in Equation [16, 49, 50] in terms of d and (H_0)

$$d = \frac{24}{\pi} * G_{sc} * (1 + 0.033 \cos\left(\frac{2\pi * nd}{365}\right) \quad (3)$$

$$H_0 = d * \left(cos\theta cos\delta sin\omega_s + \frac{\pi}{180} * \omega_s(sin\theta sin\delta)\right) \quad (4)$$

The function of relative sun shine duration S/S_0 used to compute Angstrom empirical constant or regression coefficient values of a and b based on modified Equation 5 [48, 51] as

$$a = 0.13 + 0.23\left(S/S_0\right) and\ \ b = 0.32 + 0.11\left(S/S_0\right) \quad (5)$$

The solar radiation (H) is computed based on the sunshine model employing the extraterrestrial solar radiation, H_o, relative sunshine duration S/S_0, angstrom constants (a, b) (3-4) as given in Equation (5).

$$H = \left(a + b\frac{S}{S0}\right) * H_O \quad (6)$$

The clearance index (H/H_0 = K) is the ratio of solar radiation (H) *per* extraterrestrial solar radiation (H_0) as given in Equation 6 in [48, 51]

$$H/H_0 = a + b\frac{S}{S0} \quad (7)$$

2.2.2. Multiple Linear Regressions

Multiple linear regression techniques were used to combine climatic variables (T_a, RH); (Ta, CC); (T_a, RH, CC); and (T_a, RH, CC, S/S_0) to develop regression models based on clearance (H/H_0 = k) in Equation (7-11) across nine sites. Furthermore, the regression techniques correlate the independent climatic variables with computed solar potential to predict GHI, which is given in Equation (12-16) through modified [52] as

$$k = (\beta_0 + \beta_1 T_a + \beta_2 RH + \epsilon) \quad (7)$$

$$k = \beta_0 + \beta_1 T_a + \beta_2 CC + \epsilon) \quad (8)$$

$$k = \beta_0 + \beta_1 T_a + \beta_2 RH + \beta_3 CC + \epsilon) \quad (9)$$

$$K = (\beta_0 + \beta_1 S/S_0 + \beta_2 T_a + \beta_3 RH + \beta_4 CC + \epsilon) \quad (10)$$

$$K = (\beta_0 + \beta_1 S/S_0 + \beta_2 T_a + \beta_3 RH + \beta_4 CC + \epsilon \quad (11)$$

and

$$H = (\beta_0 + \beta_1 T_a + \beta_2 RH + \epsilon) \quad (12)$$

$$H = (\beta_0 + \beta_1 T_a + \beta_2 CC + \epsilon) \quad (13)$$

$$H = (\beta_0 + \beta_1 T_a + \beta_2 RH + \beta_3 CC + \epsilon) \quad (14)$$

$$H = (\beta_0 + \beta_1 T_{max} + \beta_2 T\Delta + \beta_3 T_a + \beta_4 RH + \epsilon) \quad (15)$$

$$H = (\beta_0 + \beta_1 S/S_0 + \beta_2 T_a + \beta_3 RH + \beta_4 CC + \epsilon \quad (16)$$

Where H/H_0 is a dependent variable of clearance index, H is global solar radiation, and Ta is the average temperature, T_Δ The change of temperature T_{max} is the maximum temperature, RH is the average relative humidity, CC is the average cloud cover, and S/S_0 is the relative sunshine duration of independent climatic variables. $\beta_1, \beta_2 \ldots \beta_n$ are regression coefficient and ϵ is error.

2.2.3. Statistical Validation

The computed GHI from the sunshine model was compared with the predicted GHI using multiple linear regressions at nine climatological locations from Adama to Robe in Ethiopia. The four performance indices were employed to assess the reliability and accuracy: multiple correlations R, determination factor of R^2, Mean Bias Error (MBE), and Mean Absolute Percentage Error (MAPE).

The calculated GHI (H_i) was compared with the predicted GHI (H_j). The smaller the value, the better the accuracy of the model. The suggested model was applied to compare two data sources utilizing various statistical indicators [47-49].

These include in Equation (17-20):

$$MBE = \frac{1}{n}\sum_{i=1}^{n}(H_i - H_j) \quad (17)$$

$$MAPE = \frac{1}{n}\sum_{i=1}^{n}\left|H_i - H_j/H_i\right| * 100 \quad (18)$$

$$R = \frac{n\sum_{i=1}^{n}(H_i H_j) - (\sum_{i=1}^{n} Hi)(H_J)_j}{\left[n\sum_{i=1}^{n} H_{j_i}{}^2\right](\sum_{i=1}^{n} H_i)^2\left[n\sum_{i=1}^{n} H_i{}^2 - (\sum_{i=1}^{n} H_i)^2\right]} \quad (19)$$

$$R^2 = 1 - \frac{\sum_{i=1}^{n}(H_{reg} - H_{cal})^2}{\sum_{i=1}^{n}(H_{reg} - \dot{H})^2} \quad (20)$$

2.2.4. Spatial Interpolation Techniques

These methods incorporate computed points with a local influence that diminishes as distance increases [32]. The IDW interpolation methods forecast the average solar radiation magnitudes follow the technique given in Equation [27-32] as

$$Z_{(So)} = \sum_{i=1}^{n} \lambda_i Z_{(Si)} \quad (21)$$

Where Z(so) is the magnitude to be forecasted for sites so, n is the number of samples of calculated trial points

neighbouring the extrapolation position that might be resolved in the projection; λ_i are the weights designated to every gauged point. Z(si) is the perceived value at the site si. The weights at place si can be provided by Equation in [27-32].

$$\lambda_{i(Yo)} = \frac{d_{io}^{-p}}{\sum_{i=1}^{n} d_{io}^{-p} \sum_{i=}^{n} \lambda_{i(y_i)}} \quad (22)$$

When the length becomes greater, the weight is decreased by a negative factor of p. The amount d_{io} is the distance between the projection site, Y_o, and each of the calculated point, Y_i. The power constraint p impacts the weighting of the gauged site value on the forecasted site's value; the scaled sum of the measured location of the weights will be used for the prediction, which is equal to 1. The unknown sites of solar radiation predicting ordinary Kriging spatial interpolation are given by Equation [27-30].

$$Z_{(Xo)} = \sum_{i=1}^{n} \sigma_i Z_{(x_i)} \quad (23)$$

Where $Z(x_o)$is the forecasted magnitude of solar irradiance at unknown sites X_o; $Z(x_i)$ is the value of the calculated solar radiation z at well-known sites x_i; σ_i is the weight designated to $Z(x_i)$); and n is the number of trials for estimating.

3. Results and Discussion

3.1. Data Analysis of Meteorological Parameters for Solar Irradiance

The average magnitude of temperature, cloud cover, and relative humidity of climatic variables found from nine national meteorological stations is underscored in the study area. The climatic effects, characterized by average Temperature (Ta), Mean Cloud Cover (MCC), and average percentage Relative Humidity (RH), were analyzed in relation to global solar radiation at nine stations. The Ta, MCC, and %RH data are employed in a multiple linear regression to combine with GHI.

The minimum average annual temperature varies from 7.50C in November at Robe to 28.35^0C in April at Bahir Dar, while the maximum average annual temperature ranges from 20.3°C in October at Robe to 36.2°C in May at Dire Dawa. The mean of the temperature is the average of the minimum temperature and the maximum temperature over 13 years. The mean of the temperature value ranged from 12.7^0 °C in December at Robe to 27.9^0 °C in May-June at Dire Dewa.

The mean cloud cover value varies from the lowest 26.13% in Feb at Dire Dewa to 78.13% peak values at Nekemte in the country's western region, as depicted in Figure 3(a), (b). Similarly, the lowest average relative humidity values vary from 41.50% in February at Dire Dewa to 88.93% in July at Nekmet in the western parts based on meteorological data. The minimum values of cloud cover and relative humidity are recorded from January to May in Semiarid and arid sites, while the peak value of humidity is in the western parts of the region, as illustrated in Figure 3(c).

The cloud cover and relative humidity are generally the highest in summer and lowest in winter across nine stations. The southwest, west, and central highlands of Ethiopia region have high cloud cover and relative humidity, and the northeastern eastern semi-arid and arid parts have relatively lower cloud cover

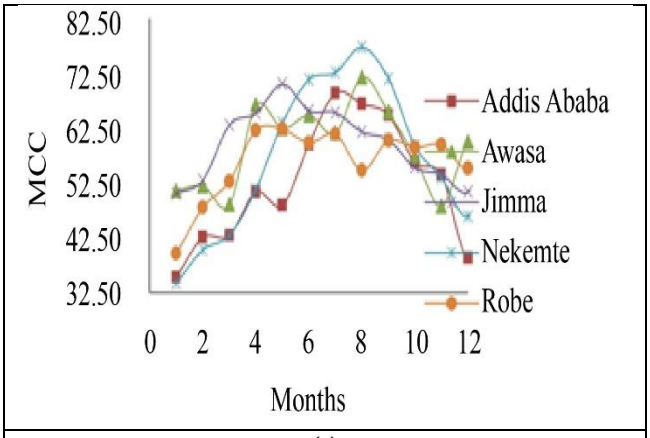

(a)

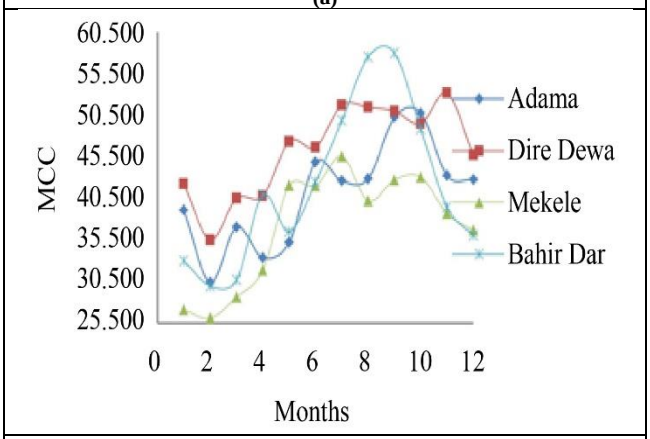

(b)

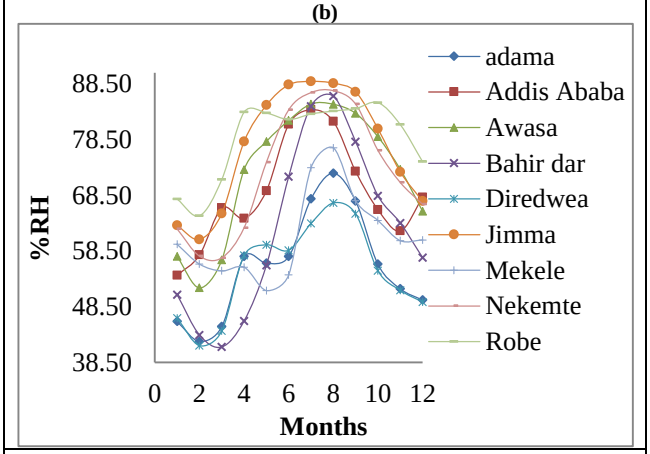

(c)

Fig. 3 (a), (b) Mean monthly cloud cover, and (c) Average relative humidity.

3.2. Climatic Effect Versus Predicted Average Solar Irradiance Using Regression Techniques

Using multiple linear regression, the climatic variable data (CC, RH) in Figure 3(a)-(c) and temperatures were correlated with computed solar radiation data. The computed monthly average solar irradiance ranged from 3.56 kWh/m²/day (July, Awasa) to 6.78 kWh/m²/day (February, Mekele). When incorporating Ta and RH, the predicted solar potential varied from 3.84 kWh/m²/day (July, Jimma) to 6.56 kWh/m²/day (February, Bahir Dar) as indicated in (Figure 4(b)). Correlating Ta and CC with the sunshine model yielded predicted GHI values of 3.83 kWh/m²/day (August, Awasa) to 6.51 kWh/m²/day (January, Mekele) as shown in Figure 4(c). Combining Ta, CC, and RH resulted in a range of 3.81 kWh/m²/day (July, Jimma) to 6.59 kWh/m²/day (February, Bahir Dar) as given in (Figure 4(d)). The analysis shows that climatic factors (RH, CC) rise from their lower values (January–March) to peak in July–August, then decline to moderate levels by September–December. Conversely, solar radiation decreases in summer (July–August) due to high humidity and cloud cover, while fluctuating between medium and high levels in spring and winter. This study confirms that average relative humidity and cloud cover significantly influence solar radiation intensity.

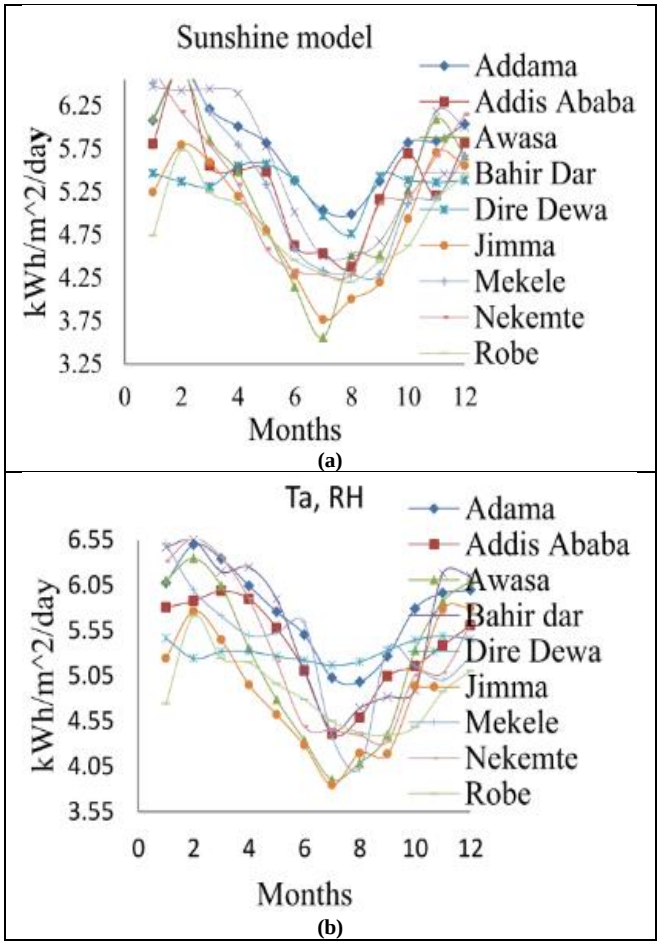

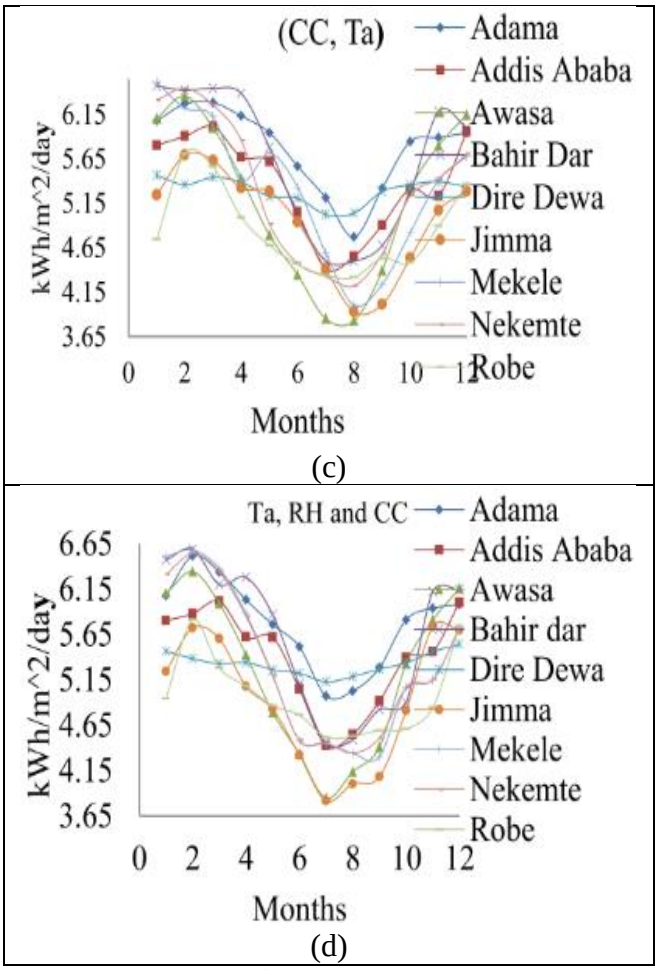

Fig. 4 Monthly average of solar radiation (a) Predicted value, and (b, c, d) after regression.

3.3. Statistical Analysis

This statistical analysis evaluated the relationship between climatic variables and solar radiation through multiple linear regression techniques, using direction correlation coefficients (R), MBE, and MAPE.

This study employed regression analysis to examine the correlation between climatic variables and solar irradiance and its clearance index (H/H_0) across nine stations. The sign coefficients (-/+) for the following variable combinations were evaluated: (i) mean air temperature (Ta) and (RH), (ii) Ta and (CC), and (iii) Ta, RH, and CC.

The analysis revealed that both RH and CC exhibited negative correlations with solar irradiance. Notably, CC demonstrated the strongest inverse relationship.

The findings confirm that climatic parameters significantly influence solar irradiance levels, with humidity and cloud cover being key factors in diminishing irradiance potential, as illustrated in Table 1.

Table 1. Comparison analysis of modelling equations and direction based on the clearance index for the nine stations

Sites	Modelling Regression Equation (Ta, RH)
Adama	$^{H}/_{H_0} = 0.422 + 0.022\mathrm{T}_a - 0.002\mathrm{RH}$
Addis Ababa	$^{H}/_{H_0} = 0.457 + 0.017\mathrm{T}_a - 0.002\mathrm{RH}$
Awasa	$^{H}/_{H_0} = 0.146 + 0.030\mathrm{T}_a - 0.000\mathrm{RH}$
Bahir Dar	$^{H}/_{H_0} = 1.035 - 0.004\mathrm{T}_a - 0.007\mathrm{RH}$
Dire Dewa	$^{H}/_{H_0} = 0.377 + 0.021\mathrm{T}_a - 0.002\ \mathrm{RH}$
Jimma	$^{H}/_{H_0} = 0.477 + 0.015\mathrm{T}_a - 0.003\mathrm{RH}$
Mekele	$^{H}/_{H_0} = 0.608 + 0.0195\mathrm{T}_a - 0.004\mathrm{RH}$
Nekemte	$^{H}/_{H_0} = 0.926 + 0.005\mathrm{T}_a - 0.005\mathrm{RH}$
Robe	$^{H}/_{H_0} = 0.890 + 0.003\mathrm{T}_a - 0.006\mathrm{RH}$
Sites	Modelling Regression Equation (CC & Ta)
Adama	$^{\mathrm{H}}/_{\mathrm{H}_0} = 0.217 - 0.004\mathrm{CC} + 0.032\mathrm{T}_\mathrm{a}$
Addis Ababa	$^{H}/_{H_0} = 0\ 620 - 0.044\mathrm{CC} + 0.010\mathrm{T}_a$
Awasa	$^{\mathrm{H}}/_{\mathrm{H}_0} = 0.257 - 0.014\mathrm{CC} + 0.027\mathrm{T}_a$
Bahir Dar	$^{H}/_{H_0} = 1.210 - 0.139\mathrm{CC} - 0.020\mathrm{T}_a$
Dire Dewa	$^{H}/_{H_0} = 0.625 - 0.065\mathrm{CC} + 0.011\mathrm{T}_a$
Jimma	$^{\mathrm{H}}/_{\mathrm{H}_0} = 0.322 - 0.018\mathrm{CC} + 0.018\mathrm{T}_a$
Mekele	$^{H}/_{H_0} = 0\ 265 - 0.036\mathrm{CC} + 0.035\mathrm{T}_a$
Nekemte	$^{H}/_{H_0} = 0\ 888 - 0.061\mathrm{CC} + 0.007\mathrm{T}_a$
Robe	$^{H}/_{H_0} = 0\ 760 - 0.081\mathrm{CC} + 0.010\mathrm{T}_a$
Site	Modelling Regression Equation (Ta, RH, and CC)
Adama	$^{H}/_{H_0} = 0.306 + 0.028\mathrm{T}_a - 0.003\mathrm{RH} - 0.029\mathrm{CC}$
Addis Ababa	$^{H}/_{H_0} = 0.586 + 0.010\mathrm{T}_a + 0.003\mathrm{RH} - 0.075\mathrm{CC}$
Awasa	$^{H}/_{H_0} = 0.256 + 0.027\mathrm{T}_a + 0.000\mathrm{RH} - 0.014\mathrm{CC}$
Bahir Dar	$^{H}/_{H_0} = 1.108 - 0.007\mathrm{T}_a - 0.006\mathrm{RH} - 0.031\mathrm{CC}$
Dire Dewa	$^{H}/_{H_0} = 0.625 + 0.009\mathrm{T}_a + 0.001\mathrm{RH} - 0.065\mathrm{CC}$
Jimma	$^{H}/_{H_0} = 0.209 + 0.014\mathrm{T}_a + 0.003\mathrm{RH} - 0.029\mathrm{CC}$
Mekele	$^{H}/_{H_0} = 0.715 + 0.017\mathrm{T}_a - 0..004\mathrm{RH} - 0.028\mathrm{CC}$
Nekemte	$^{H}/_{H_0} = 1.347 - 0.019\mathrm{T}_a + 0.001\mathrm{RH} - 0.133\mathrm{CC}$
Robe	$^{H}/_{H_0} = 0969 - 0.003\mathrm{T}_a + 0.005\mathrm{RH} - 0.028\mathrm{CC}$

Furthermore, a multiple correlation analysis was conducted to quantify the association of average air Temperature (Ta), Relative Humidity (RH), and CC with solar radiation. This analysis yielded strong correlations (R > 0.95) at some stations. The highest correlations were observed for the Ta-RH pair at Nekemte (R = 0.99), the Ta-CC pair for Nekemte (R = 0.97), and the three-variable combination (Ta, RH, CC) across multiple stations (R = 0.99). Dire Dawa was a notable exception, displaying consistently weak correlations with R-values in the range of 0.34 to 0.50 as indicated in Table 2. Finally, the climatic impact against the solar irradiance was evaluated based on MBE and MAPE. The MBE values ranged from -0.653 to 0.836 kWh/m²/day, while MAPE varied between 0.004% (Dire Dewa) to 24.52% (Mekele). Statistical tests confirmed good agreement, with minimal errors (0.004, 0.111, 0.105, and 0.344) across four climatic variable correlations as depicted in (Figure 5(a)-(b)). While some MBE values showed over- or underestimation of solar radiation,

most MAPE results (except the peak of 24.52%) fell within acceptable benchmarks. The analysis revealed that GHI increases with overestimated MBE but decreases with underestimated negative MBE values, as evidenced by higher relative humidity and cloud cover. This confirms that RH and CC negatively impact solar radiation.

Table 2. Comparison analysis of multiple correlation coefficients (R) based on H/H_0 and GHI for the nine stations

Site	Clearance index		Global-solar irradiance	
	R	R^2	R	R^2
Adama	0.909	0.826	0.98	0.96
Addis Ababa	0.751	0.564	0.78	0.61
Awasa	0.959	0.919	0.96	0.91
Bahir Dar	0.808	0.654	0.97	0.94
Dire Dew	0.561	0.314	0.45	0.2
Jimma	0.909	0.826	0.98	0.96
Mekele	0.748	0.56	0.7	0.49
Nekemte	0.845	0.714	0.99	0.98
Robe	0.657	0.432	0.89	0.78
(CC & Ta)				
Adama	0.894	0.799	0.93	0.87
Addis Ababa	0.818	0.669	0.83	0.69
Awasa	0.961	0.924	0.96	0.92
Bahir Dar	0.673	0.453	0.76	0.57
Dire Dewa	0.784	0.615	0.34	0.12
Jimma	0.883	0.78	0.82	0.67
Mekele	0.845	0.714	0.89	0.79
Nekemte	0.845	0.714	0.97	0.94
Robe	0.456	0.208	0.75	0.56
(Ta, RH and CC)				
Adama	0.925	0.855	0.98	0.96
Addis Ababa	0.838	0.702	0.83	0.7
Awasa	0.961	0.924	0.96	0.92
Bahir Dar	0.815	0.664	0.97	0.95
Dire Dewa	0.787	0.619	0.5	0.25
Jimma	0.911	0.83	0.99	0.98
Mekele	0.869	0.756	0.99	0.98
Nekemte	0.952	0.907	0.99	0.98
Robe	0.678	0.459	0.9	0.8

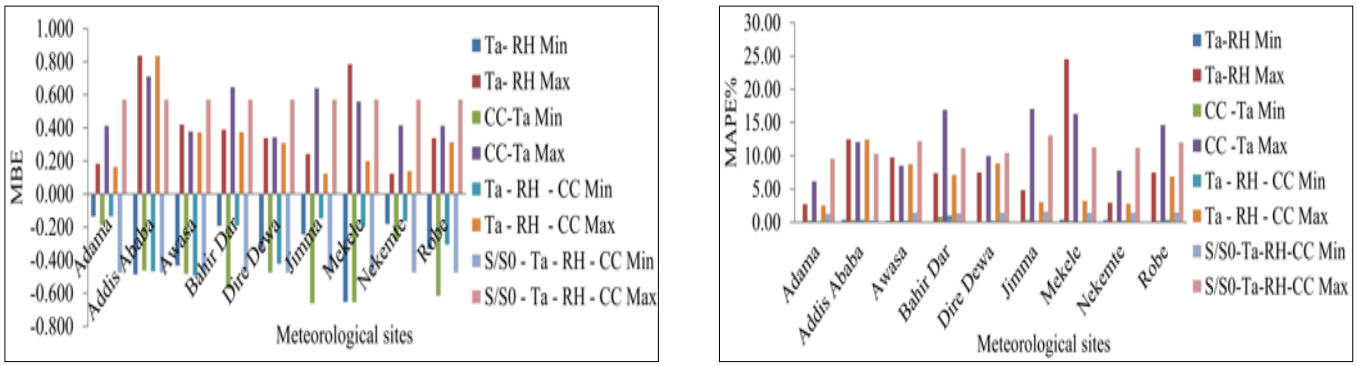

(a) **(b)**

Fig. 5 (a) Mean Bias Error, and (b) and Mean Absolute Error percentage.

3.4. The Spatial Interpolation Variability of Climatic Factors Against Global Solar Irradiance

The meteorological variability of cloud cover, relative humidity, and their corresponding global solar radiation distribution is forecasted using IDW and Kriging spatial interpolation techniques across distant and nearby regions of the country. The average cloud cover values at 44 sites varied from low CC (38 -45.5)%, Medium CC (45.5-52.5)%, to peak CC (56.5 - 63.9)% as indicated in Figure 6(a) based on kriging spatial analysis. Similarly, the average relative humidity RH of spatial distribution varies from low (0.52 to 0.90) % in different parts of the region, as displayed in Figure 6(b) based on IDW spatial interpolation. In contrary to above, the spatial exploration of solar radiation value in July varied from (4.26 to 5.66) kWh/m²/day as shown in Figure 6(c) based on Kriging interpolation while, the global solar radiation values varies from a minimum 4.07 kWh/m²/day to peak 5.94 kWh/m²/day as depicted in Figure 6(d) according to IDW exploration. Generally, spatial interpolation suggests that the western, southwestern, and some southern parts of the region experience high cloud cover and relative humidity, which reduces the global solar irradiance. In contrast, the northeastern and eastern parts of the country, with low cloud cover and relative humidity, receive higher solar radiation. The central and northern highlands, with medium cloud cover and relative humidity, result in medium to high solar radiation levels. The sparse variability in cloud cover and relative humidity constraints perceived through the two spatial interpolation techniques highlights the significant effects on global solar radiation,

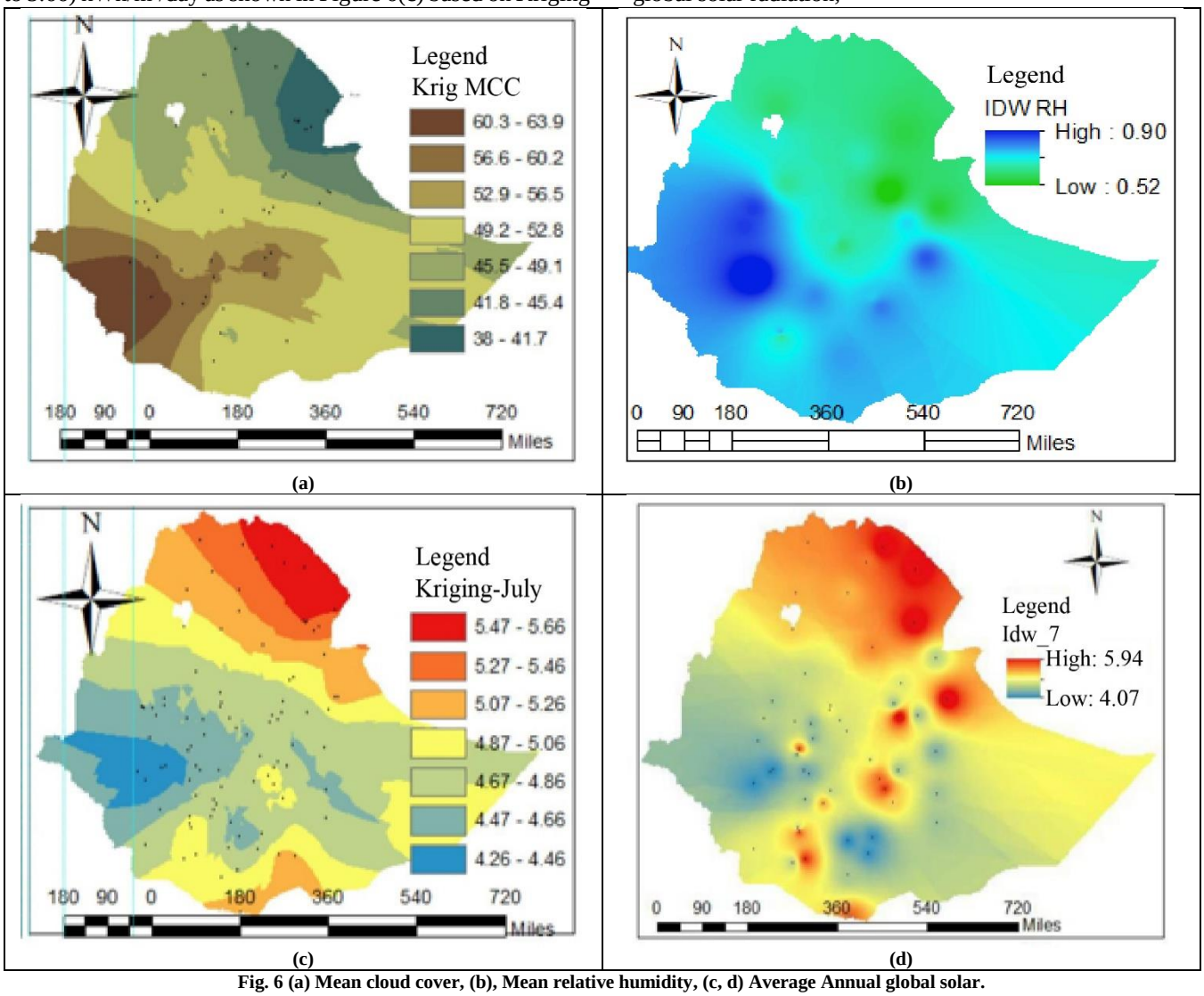

Fig. 6 (a) Mean cloud cover, (b), Mean relative humidity, (c, d) Average Annual global solar.

4. Conclusion

This study explores the correlation between meteorological parameters, such as cloud cover, relative humidity, and temperature, and global solar radiation in rural and urban areas. Various combinations of temperature, cloud cover, and humidity data with sunshine model output using regression techniques to predict solar potential. The average cloud cover and relative humidity values are low from January

to May, reach their peak in July and August, and then decline to medium levels. In contrast, solar radiation peaks between January and March due to lower cloud cover and relative humidity, then drops to its lowest values from July to August as cloud cover and humidity rise, from mid-September to December, climatic factors and solar radiation return to moderate levels with an increase in solar insolation. Throughout these patterns, cloud cover and humidity generally trend downward, while solar radiation trends upward. Integrating climatic variables into the solar potential through multiple linear regression yields predicted values that lie within the minimum and maximum computed GHI values.

Statistical analysis shows higher correlation values and lower errors, indicating good model performance. Spatially, the western, southwestern, and central regions, being more humid and cloudy, have lower solar potential, while the drier northern, northeastern, and southeastern regions exhibit higher irradiance. Strong negative correlations between climatic factors and solar irradiance highlight the significant influence of cloud cover and humidity on global horizontal irradiance. These findings demonstrate CC and RH's significant impact on global horizontal irradiance, providing critical insights for optimizing PV system design and energy planning. The future direction of the study will examine long-term climate-solar variability trends, particularly under global warming scenarios, to assess how shifting cloud and humidity patterns may alter solar potential, and exploring hybrid renewable energy systems could help mitigate solar intermittency caused by weather fluctuations. Advances in PV technology, such as bifacial panels and adaptive designs, should be evaluated for performance in high-humidity and cloudy environments.

Author Contribution

All authors participated in original drafting. V.R A, G.B.W, A.J.L, and T.T.Y: conceived and designed research. A.J.L. made a comparative analysis. A.J.L. and T.T.Y carried out the investigation. V.R A, G.B.W, and A.J.L validate the study. A.J.L., V.R.A., and T.T.Y. shared resources. All authors have reviewed, edited, read, and approved the manuscript.

Acknowledgments

The authors are grateful to the National Meteorology Agency, a seed grant from the Ministry of Education, and the ExiST project of Ethiopia.

References

[1] Sumedha R.G. Weliwaththage, and Udara S.P.R. Arachchige, "Solar Energy Technology," *Journal of Research Technology and Engineering*, vol. 1, no. 3, pp. 67-75, 2020. [Google Scholar] Publisher Link]

[2] Fiseha Mekonnen Guangul, and Girma T. Chala, "Solar Energy as Renewable Energy Source: SWOT Analysis," *2019 4th MEC International Conference on Big Data and Smart City (ICBDSC)*, Muscat, Oman, pp. 1-5, 2019. [CrossRef] [Google Scholar] [Publisher Link]

[3] B.P. Deepu, and H. Kamala, "Literature Study on Solar Energy Resources - A Geographical Analysis," *International Journal of Creative Research Thoughts*, vol. 10, no. 4, pp. f865-f879, 2022. [Google Scholar] [Publisher Link]

[4] Guruprasad Alva et al., "Thermal Energy Storage Materials and Systems for Solar Energy Applications," *Renewable and Sustainable Energy Reviews*, vol. 68, pp. 693-706, 2017. [CrossRef] [Google Scholar] [Publisher Link]

[5] Anil Kumar, and Man-Hoe Kim, "Solar Air-Heating System with Packed-Bed Energy-Storage Systems," *Renewable and Sustainable Energy Review*, vol. 72, pp. 215-227, 2017. [CrossRef] [Google Scholar] [Publisher Link]

[6] Chang Liu et al., "Historical and Future Climate Changes Impact Global Solar Photovoltaic Power Potential: Role of Key Meteorological Variables," *Atmospheric and Oceanic Science Letters*, vol. 18, no. 6, pp. 1-7, 2025. [CrossRef] [Google Scholar] [Publisher Link]

[7] Gaëtan Masson et al., "Snapshot 2024" *International Energy Agency Photovoltaic Power Systems Programme*, 2024. [CrossRef] [Publisher Link]

[8] Ankita Saxena et al., "Modelling the Global Photovoltaic Potential on Land and its Sensitivity to Climate Change," *Environmental Research Letters*, vol. 18, no. 10, pp. 1-16, 2023. [CrossRef] [Google Scholar] [Publisher Link]

[9] Yaping Hua et al., "The Impact of Climate Change on Solar Radiation and Photovoltaic Energy Yields in China," *Atmosphere*, vol. 15, no. 8, pp. 1-16, 2024. [CrossRef] [Google Scholar] [Publisher Link]

[10] N.N. Gana, and D.O. Akpootu, "Angstrom Type Empirical Correlation for Estimating Global Solar Radiation in North Eastern Nigeria," *International Journal of Engineering and Science*, vol. 2, no. 11, pp. 58-78, 2013. [Google Scholar] [Publisher Link]

[11] Reza Abdi, and Theodore Endreny, "A River Temperature Model to Assist Managers in Identifying Thermal Pollution Causes and Solutions" *Water*, vol. 11, no. 5, pp. 1-17, 2019. [CrossRef] [Google Scholar] [Publisher Link]

[12] Mathias Gustavsson, "*The Energy Report for Uganda - A 100% Renewable Energy Future by 2050*," IVL Swedish Environmental Research Institute, 2015. [Google Scholar] [Publisher Link]

[13] Anders Angstrom, "Solar and Terrestrial Radiation. Report to the International Commission for Solar Research on Actinometric Investigations of Solar and Atmospheric Radiation," *Quarterly Journal of the Royal Meteorological Society*, vol. 50, no. 210, pp. 121-126, 1924. [CrossRef] [Google Scholar] [Publisher Link]

[14] Md. Shahrukh Anis et al., "Generalized Models for Estimation of Global Solar Radiation Based on Sunshine Duration and Detailed Comparison with the Existing: A Case Study for India," *Sustainable Energy Technologies and Assessments*, vol. 31, pp. 179-198, 2019. [CrossRef] [Google Scholar] [Publisher Link]

[15] Olumide Olufemi Akinnawo et al., "Models for Prediction of Global Solar Radiation on Horizontal Surface for Akure, Nigeria," *Global Journal of Pure and Applied Sciences*, vol. 22, no. 1, pp. 43-50, 2016. [CrossRef] [Google Scholar] [Publisher Link]

[16] Ihaddadene Razika, Ihaddadene Nabila, and Mostefaoui Marouane, "Estimation of Global Solar Radiation Sunshine Duration For M'sila Region (Algeria)," *2015 3rd International Renewable and Sustainable Energy Conference (IRSEC)*, Marrakech, Morocco, pp. 1-6, 2015. [CrossRef] [Google Scholar] [Publisher Link]

[17] Meher Chelbi, Yves Gagnon, and Jompob Waewsak, "Solar Radiation Mapping using Sunshine Duration based Models and Interpolation Techniques: Application to Tunisia Energy Conversion and Management," *Energy Conversion and Management*, vol. 101, pp. 203-215, 2015. [CrossRef] [Google Scholar] [Publisher Link]

[18] Teshome B. Kotu et al., *Prediction of Global Solar Radiation based on Sunshine Hours in Ethiopia's Amhara Region*, Advancement of Science and Technology, pp. 1-31, 2023. [CrossRef] [Google Scholar] [Publisher Link]

[19] Qingwen Zhang et al., "Comparative Analysis of Global Solar Radiation Models in Different Regions of China," *Advances in Meteorology*, vol. 2018, no. 1, pp. 1-21, 2018. [CrossRef] [Google Scholar] [Publisher Link]

[20] D.O. Akpootu, and Y.A. Sanusi, "A New Temperature-Based Model for Estimating Global Solar Radiation in Port-Harcourt, South-South Nigeria," *The International Journal of Engineering and Science*, vol. 4, no. 1, pp. 63-73, 2015. [Google Scholar] [Publisher Link]

[21] Tegenu Argaw Woldegiyorgis, "Prediction and Comparison of Daily Global Solar Radiation using Meteorological Data," *Applied Journal of Environmental Engineering Science*, vol. 6, no. 3, pp. 310-324, 2020. [CrossRef] [Google Scholar] [Publisher Link]

[22] Girma Dejene Nage, "Estimation of Monthly Average Daily Solar Radiation from Meteorological Parameters: Sunshine Hours and Measured Temperature in Tepi, Ethiopia," *International Journal of Energy and Environmental Science*, vol. 3, no. 1, pp. 19-26, 2018. [CrossRef] [Google Scholar] [Publisher Link]

[23] Kun Lan et al., "The Applicability of Sunshine-Based Global Solar Radiation Models Modified with Meteorological Factors for Different Climate Zones of China," *Frontiers in Energy Research*, vol. 10, pp. 1-15, 2023. [CrossRef] [Google Scholar] [Publisher Link]

[24] Sayed Saber Sharifi, Vahid Rezaverdinejad, and Vahid Nourani, "Estimation of Daily Global Solar Radiation using Wavelet Regression Ann, Gep and Empirical Models: A Comparative Study of Selected Temperature Based Approaches," *Journal of Atmospheric and Solar-Terrestrial Physics*, vol. 149, pp. 131-145, 2016. [CrossRef] [Google Scholar] [Publisher Link]

[25] Tegenu Argaw Woldegiyorgis et al., "Estimating Solar Radiation using Artificial Neural Networks: A Case Study of Fiche, Oromia, Ethiopia," *Cogent Engineering*, vol, 10, no. 1, pp. 1-13, 2023. [CrossRef] [Google Scholar] [Publisher Link]

[26] Neelamegam Premalatha, and Amirtham Valan Arasu, "Prediction of Solar Radiation for Solar Systems by using ANN Models with Different Back Propagation Algorithm," *Energy*, vol. 14 no. 3, pp. 206-214, 2016. [CrossRef] [Google Scholar] [Publisher Link]

[27] Daniel N. Katongole et al., "Spatial and Temporal Solar Potential Variation Analysis in Uganda Using Measured Data," *Tanzania Journal of Science*, vol. 49, no. 1, pp. 1-14, 2023. [CrossRef] [Google Scholar] [Publisher Link]

[28] Leonardo Ramos Emmendorfer, and Graçaliz Pereira Dimuro, "A Novel Formulation for Inverse Distance Weighting from Weighted Linear Regression, Netherlands," *International Conference on Computational Science*, Amsterdam, The Netherlands, pp. 576-589, 2020. [CrossRef] [Google Scholar] [Publisher Link]

[29] S. Persiano et al., "Changes in Seasonality and Magnitude of Sub-Daily Rainfall Extremes in Emilia-Romagna and Potential Influence on Regional Rainfall Frequency Estimation," *Journal of Hydrology: Regional Studies*, vol. 32, pp. 1-17, 2020. [CrossRef] [Google Scholar] [Publisher Link]

[30] Kazhal Masroor et al., "Spatial Modelling of PM2.5 Concentrations in Tehran using Kriging and Inverse Distance Weighting (IDW) Methods," *Journal of Air Pollution and Health*, vol. 5, no. 2, pp. 89-96, 2020. [CrossRef] [Google Scholar] [Publisher Link]

[31] Tao Chen et al., "Comparison of Spatial Interpolation Schemes for Rainfall Data and Application in Hydrological Modelling," *Water*, vol. 9, no. 5, pp. 1-18, 2017. [CrossRef] [Google Scholar] [Publisher Link]

[32] Xinyuan Hou et al., "Climate Change Impacts on Solar Power Generation and its Spatial Variability in Europe Based on CMIP6," *Earth System Dynamics*, vol. 12, no. 4, pp. 1099-1113, 2021. [CrossRef] [Google Scholar] [Publisher Link]

[33] Z. Abbas et al., "Effect of Ambient Temperature and Relative Humidity on Solar PV System Performance: A Case Study of Quaid-e-Azam Solar Park, Pakistan," *Sindh University Research Journal - SURJ (Science Series)*, vol. 49, no. 4, pp. 721-726, 2017. [Google Scholar] [Publisher Link]

[34] Ceyda Aksoy Tırmıkçı, Cenk Yavuz, and Talha Enes Gümüş, "Investigating the Effects of Temperature and Relative Humidity on Performance Ratio of a Grid Connected Photovoltaic System," *Academic Platform Journal of Engineering and Science*, vol. 9, no. 3, pp. 427-432, 2021. [CrossRef] [Google Scholar] [Publisher Link]

[35] S. Ayegba Abdullahi, Musa Abdul, and Adejoh Joshua, "Impacts of Relative Humidity and Mean Air Temperature on Global Solar Radiations of Ikeja, Lagos, Nigeria," *International Journal of Scientific and Research Publications*, vol. 7, no. 2, pp. 315-319, 2017. [Google Scholar] [Publisher Link]

[36] Andrea de Almeida Brito, Heráclio Alves de Araújo, and Gilney Figueira Zebende, "Detrended Multiple Cross Correlation Coefficient Applied to Solar Radiation, Air Temperature and Relative Humidity," *Scientific Reports*, vol. 9, no. 1, pp. 1-10, 2019. [CrossRef] [Google Scholar] [Publisher Link]

[37] Brian R. Burg et al., "Effects of Radiative Forcing of Building Integrated Photovoltaic Systems in Different Urban Climates," *Solar Energy*, vol. 147, pp. 399-405, 2017. [CrossRef] [Google Scholar] [Publisher Link]

[38] Md Rokonuzzaman, and Mohammad Maksudur Rahman, "Effect of Cloud Coverage on Sunshine, Humidity, Rainfall and Temperature for Different Weather Stations in Bangladesh: A Panel Analysis," *IOSR Journal of Environmental Science, Toxicology and Food Technology (IOSR-JESTFT)*, vol. 11, no. 3, pp. 1-6, 2017. [Google Scholar] [Publisher Link]

[39] Chen Chunmei, Zhong Ke, and Chen Yonghang, "Effects of Clouds on Solar Radiation over Typical City in Arid Area," *Arid Zone*, vol. 35, no. 2, pp. 436-443, 2018. [Google Scholar]

[40] Hassan Gholami, and Harald Nils Røstvik, "The Effect of Climate on the Solar Radiation Components on Building Skins and Building Integrated Photovoltaic (BIPV) Materials," *Energies*, vol. 14, no. 7, pp. 1-15, 2021. [CrossRef] [Google Scholar] [Publisher Link]

[41] Mfongang Erim Agbor et al., "Potential Impacts of Climate Change on Global Solar Radiation and PV Output using the CMIP6 Model in West Africa," *Cleaner Engineering and Technology*, vol. 13, pp. 1-20, 2023. [CrossRef] [Google Scholar] [Publisher Link]

[42] Derrick Kwadwo Danso et al., "A CMIP6 Assessment of the Potential Climate Change Impacts on Solar Photovoltaic Energy and its Atmospheric Drivers in West Africa," *Environmental Research Letters*, vol. 17, no. 4, pp. 1-13, 2022. [CrossRef] [Google Scholar] [Publisher Link]

[43] Yuwen Si et al., "Effects of Single-Layer Low Clouds on the Surface Solar Radiation in East Asia," *Solar Energy*, vol. 224, pp. 1099-1106, 2021. [CrossRef] [Google Scholar] [Publisher Link]

[44] Ashebir Dingeto Hailu, and and Desta Kalbessa Kumsa, "Ethiopia Renewable Energy Potentials and Current State," *AIMS Energy*, vol. 9, no. 1, pp. 1-14, 2021. [CrossRef] [Google Scholar] [Publisher Link]

[45] Solomon Feleke et al., "Feasibility and Potential Assessment of Solar Resources: A Case Study in North Shewa Zone, Amhara, Ethiopia," *Energies*, vol. 16, no. 6, pp. 1-15, 2023. [CrossRef] [Google Scholar] [Publisher Link]

[46] Natei Ermias Benti et al., "Estimation of Global Solar Radiation using Sunshine-based Models in Ethiopia," *Cogent Engineering*, vol. 9, no. 1, pp. 1-25, 2022. [CrossRef] [Google Scholar] [Publisher Link]

[47] Fitsum Bekele et al., Revised Meteorological Station Network Master Plan For 2021-2030, National Meteorological Agency, 2023. [Online]. Available: https://www.ethiomet.gov.et/publications/revised-meteorological-station-network-master-plan-for-2021-2030/

[48] John A. Duffie, William A. Beckman, and Nathan Blair, *Solar Engineering of Thermal Processes, Photovoltaic and Wind*, John Wiley & Sons, Inc., 2020. [Cross Ref] [Google Scholar] [Publisher Link]

[49] Tihomir Betti et al., "A Comparison of Models for Estimating Solar Radiation from Sunshine Duration in Croatia," *International Journal of Photoenergy*, vol. 2020, no. 1, pp. 1-14, 2020. [Cross Ref] [Google Scholar] [Publisher Link]

[50] Milan Despotovic et al., "Review and Statistical Analysis of Different Global Solar Radiation Sunshine Models," *Renewable and Sustainable Energy Reviews*, vol. 52, pp. 1869-1880, 2015. [Cross Ref] [Google Scholar] [Publisher Link]

[51] Muhammed A. Hassan et al., "Independent Models for Estimation of Daily Global Solar Radiation: A Review and A Case Study," *Renewable and Sustainable Energy Reviews*, vol. 82, pp. 1565-1575, 2018. [Cross Ref] [Google Scholar] [Publisher Link]

[52] Rahul G. Makade, and Basharat Jamil, "Statistical Analysis of Sunshine-Based Global Solar Radiation (GSR) Models for Tropical Wet and Dry Climatic Region in Nagpur, India: A Case Study," *Renewable and Sustainable Energy Reviews*, vol. 87, pp. 23-42, 2018. [Cross Ref] [Google Scholar] [Publisher Link]

[53] S. Ibrahim et al., "Linear Regression Model in Estimating Solar Radiation in Perlis," *Energy Procedi*a, vol. 18, pp. 1402-1412, 2012. [Cross Ref] [Google Scholar] [Publisher Link]

[54] Stephen A. Klein et al., *Low-Cloud Feedbacks from Cloud-Controlling Factors: A Review, Surveys in Geophysics*, vol. 38, pp. 1307-1329, 2017. [Cross Ref] [Google Scholar] [Publisher Link]